Characterization of Apolipoprotein A-I Structure Using a Cysteine-Specific Fluorescence Probe†

M. Alejandra Tricerri,‡ Andrea K. Behling Agree,‡ Susana A. Sanchez,§ and Ana Jonas*,‡

Department of Biochemistry and Laboratory for Fluorescence Dynamics, University of Illinois at Urbana-Champaign Urbana, Illinois 61801

Received June 21, 2000

ABSTRACT: Two new Cys mutants of proapolipoprotein A-I, D9C and A232C, were created and expressed in *Escherichia coli* systems. Specific labeling with the thiol-reactive fluorescence probe, 6-acryloyl-2-dimethylaminonaphthalene (acrylodan), was used to study the structural organization and dynamic properties of the extreme regions of human apolipoprotein A-I (apoA-I) in lipid-free and lipid-bound states. Spectroscopic approaches, including circular dichroism and various fluorescence methods, were used to examine the properties of the mutant proteins and of their covalent adducts with the fluorescence probe. The mutations themselves had no effect on the structure and stability of apoA-I in the lipid-free state and in reconstituted HDL (rHDL) complexes. Furthermore, covalent modification with acrylodan did not alter the properties of the apoA-I variants in the lipid-bound state nor in the lipid-free A232C mutant, but it affected the structure and local stability of the lipid-free protein in the D9C mutant. Fluorescence results using the acrylodan probe confirmed a well-organized structure in the N-terminal region of apoA-I. Also, they suggested a three-dimensional structure in the C-terminal region, stabilized by protein−protein contacts. When Trp residues and acrylodan were used as donor−acceptor pairs for fluorescence resonance energy transfer (FRET), average distances could be measured. Both intensity and lifetime changes of the Trp emission indicated a protein folding in solution that brings the C-terminus of the protein near the Trp residues in the N-terminal half of the sequence. Also, the N- and C-terminal domains of apoA-I appeared to be near each other in rHDL having two apoA-I per particle.

Apolipoprotein A-I (apoA-I),[1] the major protein component of high-density lipoproteins (HDL), determines the structure and function of this lipoprotein class. In addition to binding phospholipids, and solubilizing cholesterol and cholesterol esters, apoA-I is the principal activator of the lecithin cholesterol acyltransferase reaction in plasma (*1*), a modulator of lipid transfers and HDL rearrangements by cholesterol ester and phospholipid transfer proteins (*2*, *3*), and a ligand for cell surface receptors (*4*).

The primary sequence of apoA-I contains repeating 22- and 11-amino acid segments that form amphipathic helices that bind to phospholipids and stabilize HDL in aqueous solution (*5*). In fact, lipid-bound apoA-I contains 70−80% α-helical structure, while lipid-free apoA-I, in low ionic strength buffers at physiologic pH, has about 50% α-helical structure (*6*). The tertiary, high-resolution structure of apoA-I under these physiologic conditions is unknown. A crystal structure of a 44−243 amino acid fragment of apoA-I, obtained in high salt, shows a highly α-helical, extended structure that curves into a horseshoe shape for each monomer in an overlapping, circular tetramer (*7*). While this structure confirms the existence of amphipathic helices and the ability of lipid-free apoA-I to self-associate at high concentrations (>0.1 mg/mL), the actual three-dimensional organization of the helices does not agree with many known facts about the more physiologic lipid-free or lipid-bound apoA-I structures.

A fruitful approach to the study of the structure and function of apoA-I in solution and in reconstituted HDL (rHDL) has been the production of apoA-I mutants with deletions in their sequence or with specific point mutations (*8*−*11*). In this study, we have introduced Cys residues, which are not found in the normal sequence of apoA-I. The

† This work was supported by NIH Grant HL-16059 to A. Jonas and a predoctoral fellowship from the American Heart Association, Illinois Affiliate, to A. Behling Agree.

* To whom correspondence should be addressed. Dr. Ana Jonas, Department of Biochemistry, College of Medicine, University of Illinois at Urbana-Champaign, 506 South Mathews Avenue, Urbana, IL 61801. Telephone: (217) 333-0452. Fax: (217) 333-8868. E-mail: a-jonas@uiuc.edu.

‡ Department of Biochemistry.

§ Laboratory for Fluorescence Dynamics.

[1] Abbreviations: apoA-I, apolipoprotein A-I; HDL, high-density lipoproteins; Ac, acrylodan, 6-acryloyl-2-dimethylaminonaphthalene; D9C and A232C, mutant forms of recombinant proapoA-I containing Cys residues at positions 9 and 232 of the apoA-I sequence; D9C-Ac and A232C-Ac, mutants covalently and specifically labeled with acrylodan; DPPC, dipalmitoylphosphatidylcholine; DMPC, dimyristoylphosphatidylcholine; PMSF, phenylmethylsulfonylfluoride; GndHCl, guanidine hydrochloride; DTT, dithiothreitol; TCEP, tris-(2-carboxyethyl)phosphine hydrochloride; rHDL, reconstituted HDL; τ, fluorescence lifetime; WMF, wavelength of maximum fluorescence; WT, WT-proapoA-I, wild-type recombinant apoA-I containing a 6-amino acid pro segment; ϕ, rotational correlation time; apoA-II, apolipoprotein A-II; apoE, apolipoprotein E; apoA-I-Milano, naturally occurring Cys mutant of apoA-I (R173C); apoA-I-Paris, naturally occurring Cys mutant of apoA-I (R151C).

10.1021/bi0014251 CCC: $19.00
Published on Web 11/02/2000

mutations are located near the N-terminus (D9C) or near the C-terminus (A232C) and are the sites for specific labeling with a thiol-reactive probe, acrylodan (Ac). This fluorescence probe is used to examine the physical environments and motions of these regions that are structurally and functionally important in apoA-I. The N-terminus of apoA-I is a highly conserved region with a predicted G-type helix that rearranges its structure dramatically upon binding to lipids (*12*). The C-terminus is thought to have little structure in solution (*13*) but is important in the initial binding of apoA-I to lipid bilayers (*14*) and to cell membranes (*15*) and for the stabilization of lipid-bound apoA-I (*13*).

The objectives of this study were to examine the structure of the N- and C-terminal regions of apoA-I and to determine whether the C-terminus is extended and flexible as suggested by Roberts et al. (*16*) and Davidson et al. (*13*). In addition, using fluorescence resonance energy transfer, we wished to estimate the distances between the Trp residues and the N- and C-terminal regions of apo A-I in lipid-free and lipid-bound states.

MATERIALS AND METHODS

Materials. Human plasma apoA-I was purified from blood plasma purchased from the Champaign County Blood Bank, Regional Health Center, as described previously (*17*). Dipalmitoylphosphatidylcholine (DPPC), dimyristoylphosphatidylcholine (DMPC), phenylmethylsulfonylfluoride (PMSF), and sodium cholate were purchased from Sigma Chemical Co.; ultrapure guanidine hydrochloride (GndHCl) and dithiothreitol (DTT) were obtained from Boehringer Mannheim; 6-acryloyl-2-dimethylaminonaphthalene (acrylodan, Ac) and tris-(2-carboxyethyl)phosphine hydrochloride (TCEP) were purchased from Molecular Probes. Kanamycin sulfate and IPTG were obtained from CalBiochem.

Methods. Site-Directed Mutagenesis. The gene for human proapoA-I was modified so that it contained the unique restriction sites *Nco*I and *Hin*dIII. The proapoA-I cDNA (gift from Dr. J. Gordon, Washington University) was subcloned into the vector pBluescript KS (Stratagene). This plasmid was used for mutagenesis. The D9C variant was constructed using the megaprimer method of PCR-based site-directed mutagenesis. The A232C variant was constructed using the Quickchange method (Stratagene). The sequences for the coding strands of the mismatch primers were (mismatch codons are underlined) D9C, 5N-CCC TGG TGC CGA GTG AAG GAC CTG GCC ACT GTG TAC-3N; A232C, 5N-AAG GTC AGC TTC CTG AGC TGT CTC GAG GAG TAC ACT AAG-3N. The mutations were confirmed by DNA sequencing at the Biotechnology Center (University of Illinois, Urbana-Champaign).

Overexpression and Purification. The mutant and the WT proapoA-I cDNAs were subcloned into the pET-28a 5.8-kB expression plasmid, which was then transformed into BLR (DE3) *E. coli* cells (Novagen). An overnight culture (10 mL) was used to inoculate 6 L of LB broth containing 30 μg/mL kanamycin. Cells were grown at 37 °C in a shaking incubator to an $A_{600\ nm}$ of 0.5, then IPTG (0.8 mM) was added to induce expression of proapoA-I, and the cells were allowed to grow for 2.5−3 h at 37 °C. Cells were harvested by centrifugation at 5000 rpm for 10 min, and the pellet was stored at −80 °C. The cells were resuspended in buffer A containing 50 mM Tris-HCl, pH 7.9, 0.5 mM EDTA, 50 mM NaCl, 5% glycerol, 0.1 mM PMSF, 0.1 mM sodium meta-bisulfite, and 6.5 mM DTT and lysed by intermittent sonication over 3 min, followed by exposure to 0.2% deoxycholic acid for 10 min. Inclusion bodies were pelleted by centrifugation at 18 000 rpm for 20 min. A 20% $(NH_4)_2SO_4$ precipitation was performed on the soluble fraction, followed by a 30% $(NH_4)_2SO_4$ precipitation on the supernatant from the 20% cut. The proapoA-I was pelleted by centrifugation, and the pellet was resuspended in buffer B containing 10 mM Tris-HCl, pH 8.0, 0.1 mM EDTA, 0.1 mM PMSF, 0.1 mM sodium meta-bisulfite, and 6.5 mM DTT and applied to a Phenyl Sepharose column (Pharmacia, CL-4B) at 4 °C. Weakly bound proteins were removed by washing the column with buffer B. Elution was performed using a stepwise gradient from 100% buffer B to buffer B containing 45, 60, and 70% ethylene glycol. The fractions containing the highest amounts of proapoA-I estimated by SDS−PAGE and $A_{280\ nm}$ were pooled and dialyzed against 5 mM NH_4 bicarbonate. The dialyzed protein was lyophilized and stored under N_2 at −20 °C. The inclusion bodies were solubilized over 4 h in buffer B containing 6 M GndHCl. Insoluble debris was removed by centrifugation at 18 000 rpm for 15 min, and the supernatant was dialyzed against buffer B. After centrifugation, the inclusion body fraction was purified on a Phenyl Sepharose column using the same conditions just described.

Labeling of the Mutants with Acrylodan (Ac). Acrylodan (20 mM) in dimethylformamide was added to the mutants in 0.1 M phosphate, pH 7.0 buffer containing 0.4 mM TCEP. The probe was added in small volumes to a final molar ratio of 5:1 Ac/protein. The reaction mixtures were stirred at room temperature, in the dark for 2 h. The kinetics of labeling were followed with a hand-held UV lamp by the development of a green-blue fluorescence. Labeled proteins were passed through a PD-10 column to remove unreacted Ac. Plasma apoA-I was reacted alongside the mutants to detect nonspecific labeling. The efficiency of Ac binding to the thiol group was determined using absorbance at 390 nm and $\epsilon = 20\ 200\ cm^{-1}\ M^{-1}$ (*18*), and protein concentration was determined by the Lowry assay (*19*).

Preparation of rHDL Particles and Solubilization of DMPC Liposomes. The ability of the apoA-I mutants and their adducts with Ac to bind phospholipids was examined by two methods: formation of reconstituted HDL (rHDL) and solubilization of dimyristoylphosphatidylcholine (DMPC) multilamellar liposomes.

Reconstituted HDL were prepared by the sodium cholate dialysis method using DPPC/protein/sodium cholate molar ratios of 100:1:150, which have been shown to result primarily in 96-Å discoidal particles containing two molecules of apoA-I per complex (*20*). Each reaction mixture contained 2−4 mg of protein in a maximum volume of 2.5 mL of 10 mM Tris buffer, pH 8.0, 0.15 M NaCl, 1 mM NaN_3, and 0.1 mM EDTA (buffer C). After removal of the sodium cholate by extensive dialysis, samples were concentrated using Centriprep 30 Amicon membranes subjected to low speed centrifugation. The rHDL preparations were purified further by passage through two columns (Superose 6 and Superdex 200 HR 10/30) in tandem using a Pharmacia FPLC System. The columns were equilibrated with buffer C, and the elution was performed at a flow rate of 0.3 mL/min. The

homogeneity and hydrodynamic diameters of the rHDL were estimated by native (8−25%) polyacrylamide gel electrophoresis on a Pharmacia Phast System. All apoA-I variants formed 96-Å rHDL particles efficiently and in high yields.

The rate of lysis of DMPC multilamellar liposomes by the apoA-I variants was observed by the decrease in light scattering at $A_{325\ nm}$, using the experimental conditions described previously (*21*).

Secondary Structure and Stability Determination. The average α-helical content of apoA-I variants as well as the free energy of unfolding was determined by far UV circular dichroism. Spectra were recorded with a Jasco J-720 spectropolarimeter at 25 °C using a 0.1-cm quartz cuvette. Sample concentrations for the lipid-free proteins were 0.06 mg/mL in 0.1 M phosphate buffer, pH 8.0, to prevent self-association. The concentration of the rHDL samples was 0.1 mg/mL in terms of protein. The percent of α-helix was calculated from the ellipticity at 222 nm by the empirical expression of Chen et al. (*22*). The unfolding of the lipid-free proteins was analyzed by incubation of the proteins with increasing concentrations of GndHCl, at 4° C for at least 2 h prior to measurement of ellipticity at 222 nm. The lipid-bound proteins in rHDL particles were denaturated by incubating the samples with GndHCl at 4° C for 72 h to reach equilibrium. The thermodynamic parameters of unfolding of the apoA-I variants were calculated from the spectral values. Data in the form of apparent fraction of unfolded protein (F_{app}) versus GndHCl concentration were fitted to an equation derived by considering a two-state process from native to unfolded. The dependence of $\Delta G°$ on GndHCl concentration is approximated by a linear equation (*23*):

$$\Delta G° = \Delta G°_{H_2O} + m[\text{GndHCl}] \quad (1)$$

where m is a coefficient that is thought to report on the cooperativity of the unfolding transition and the exposure of hydrophobic surface area during unfolding (*24*).

Fluorescence Spectroscopy. Steady-State Measurements. For all fluorescence studies, the concentration of lipid-free proteins was lower than 0.1 mg/mL (to prevent self-association) and 0.1 mg/mL for rHDL. Uncorrected emission spectra were recorded with an ISA SPEX Fluoromax-photon counting spectrofluorometer, using 295-nm light to excite Trp fluorescence and 360-nm light to excite Ac. When denaturing the proteins with the appropriate aliquots of 6.4 M GndHCl, the shifts in the WMF or fluorescence intensity changes were measured after an incubation of 2 h (for the lipid-free proteins) or after 72 h for the rHDL. Trp in the unlabeled variants was excited as described above, and emission was collected between 305 and 450 nm. Acrylodan-labeled mutants were excited at 360 nm, collecting emission from 400 to 600 nm to examine the acrylodan residue alone. For energy transfer experiments, the labeled proteins were excited at 295 nm, and emission was collected from 305 to 600 nm. Spectra were corrected with blanks containing identical concentrations of GndHCl for background noise.

Time-Resolved Measurements. Time-resolved fluorescence (lifetime) and polarization measurements were performed using a cross correlation phase and modulation fluorometer. For the measurement of Trp fluorescence, an excitation wavelength of 295 nm from the output of a ND:YAG-pumped Rhodamine 6G dye laser (Coherent, Palo Alto, CA) was employed. The emission was observed through a long pass filter (WG 320, Schott) and a U-330 band-pass filter to remove scattered light. *p*-Terphenyl (lifetime, $\tau = 1.05$ ns) in absolute ethanol was used as a lifetime reference. The phase and modulation data were collected across a harmonic range of 10−200 MHz. For the measurement of acrylodan fluorescence, the excitation wavelength was 345 nm from the output of a ND:YAG-pumped DCM dye laser (Coherent, Palo Alto, CA). The sample emission was observed through a Schott KV 399 long pass filter to eliminate scattered excitation light and transmit fluorescence above 375 nm. POPOP [1,4-bis(5-phenyloxazol-2-yl)benzene] was used as the lifetime standard (1.35 ns). A harmonic range of 20−200 MHz was used in this case.

To eliminate polarization effects, lifetime data were collected under magic angle conditions, such that the excitation beam was polarized normal to the laboratory plane, and the emission was viewed through a polarizer set to 55° (*25*). Samples were thermostated at 20 °C during data acquisition.

Data were analyzed using GLOBALS Unlimited TM software (*26*) for multiple lifetime and correlation time components with a constant error of the modulation and phase data fixed at 0.02 and 0.2°, respectively. Trp fluorescence data were analyzed using a model of three discrete lifetimes and two rotational correlation times; a different model of two lifetimes and two rotational correlation times was used for the Ac measurements. The average lifetimes $<\tau>$ were then calculated by summing the products of the lifetimes and the corresponding fractional intensities.

Energy Transfer Determination. The efficiency of energy transfer (E) as a function of distance (R), between two probes (Trp and Ac) was determined from fluorescence lifetimes or intensities as follows (*27*):

$$E = 1 - (\tau_{da}/\tau_d) = 1 - (F_{da}/F_d) = R^6{}_o/(R^6{}_o + R^6) \quad (2)$$

where R_o represents the distance at which energy transfer is 50% efficient; τ_{da} and F_{da} are the fluorescence lifetime and the intensity of the donor in the presence of acceptor; τ_d and F_d are the donor lifetime and intensity in the absence of acceptor. The value of R_o for energy transfer from Trp to Ac in a protein is 2.7 nm (*28*).

RESULTS

Overexpression and Purification of Recombinant Proteins. The *E. coli* expression system combined with the purification procedures of this study gave good yields of mutant proapoA-I and WT proapoA-I (∼5−10 mg of pure proapoA-I mutants/6 L of cell culture). The degree of purity of the mutant proteins was in excess of 95%, as shown by SDS−PAGE (see Figure 1, panel A). Presence of reduced Cys residues in the D9C and A232C mutants was confirmed by the specific and stoichiometric reaction of the thiol probe, acrylodan (Ac), with each of the mutant proteins. The labeling efficiency ranged from 0.8 to 1.0 for different preparations, with a nonspecific labeling of the control plasma apoA-I of only 5−10%, under the same reaction conditions.

Structure of Variant Forms of ApoA-I. Prior to the analysis and interpretation of the fluorescence results with the Ac-labeled mutants, we set out to establish the effects of

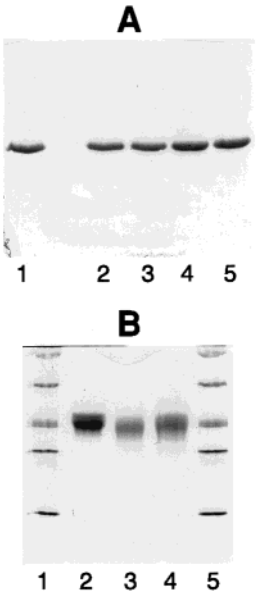

FIGURE 1: (A) SDS−PAGE of purified proteins. Lane 1, plasma apoA-I; lanes 2 and 4, D9C variant; lanes 3 and 5, A232C variant. (B) Nondenaturing gradient gel (8−25%) of standard proteins (lanes 1 and 5) and reconstituted HDL (100:1, DPPC/apoA-I variant) with plasma apoA-I (lane 2), D9C-Ac variant (lane 3), and A232C-Ac variant (lane 4).

Table 1: Characterization of the ApoA-I Variants in Lipid-Free and rHDL Forms

	lipid-free			rHDL
protein	WMF Trp[a] (nm)	α-helix[b] (%)	ΔG^o denat (kcal/mol)	WMF Trp[a] (nm)
WT	334 ± 2	57 ± 7	2.5 ± 0.3	333 ± 2
D9C	334	50	2.5	333
A232C	334	50	3.0	333
D9C-Ac	334	46	2.5	333
A232C-Ac	334	52	2.7	334

[a] Wavelength of maximum fluorescence is the average for the five Trp residues in the recombinant forms of proapoA-I. [b] The α-helix content was calculated from CD measurements at 222 nm using the expression of Chen et al. (*22*). Protein concentrations were determined by the Lowry et al. (*19*) method. [c] From CD molar ellipticity values, measured at equilibrium as a function of GndHCl concentrations, fitted to the equation for $\Delta G°$ of denaturation (*23*, *24*).

introducing Cys residues into proapoA-I, and of covalently modifying the Cys residues with acrylodan, on the overall structure and lipid-binding properties of apoA-I.

The effects on proapoA-I structure of the mutations and of the covalent labeling were analyzed by circular dichroism spectroscopy (determination of α-helix content and free energy of unfolding ($\Delta G°$) and fluorescence spectroscopy [wavelength of maximum fluorescence (WMF) of Trp residues], lifetimes and rotational correlation times).

Table 1 lists the α-helix contents and free energies of denaturation of the lipid-free mutants (D9C and A232C) and acrylodan-labeled variants (D9C-Ac and A232C-Ac) as compared with wild-type (WT) protein. These parameters are similar for all the apoA-I variants, with the possible exception of D9C-Ac, which may have a lower content of α-helical structure (46%). The free energies of denaturation were determined from the values of ellipticity at 222 nm as a function of GndHCl concentration. Both the free-energy values and the cooperativity parameter *m* (not shown) are comparable for all the apoA-I variants in lipid-free form. On the basis of these results, the introduction of the Cys mutations and the Ac probe into the A232C mutant have little or no effect on the secondary, α-helical structure of apoA-I and its stability in aqueous solution. Introduction of the Ac probe into the N-terminal, D9C mutant may alter the secondary structure of the protein without affecting its stability.

Similarly, the effects of the mutations and the probe attachment were examined following the fluorescence of Trp residues in all the apoA-I variants to detect any changes in the environments of the Trp residues and the stability of the three-dimensional structures of the proteins in their N-terminal halves. The average WMF of the Trp residues is identical for the lipid-free forms of all the apoA-I variants (334 nm) indicating that the low polarity of the Trp environments of apoA-I is unchanged when Cys residues are introduced and are further reacted with acrylodan (see Table 1). The free energies of denaturation calculated from the variation of these parameters with GndHCl, ranged from 2.6 to 3.2 kcal/mol (not shown), in close agreement with the results obtained from CD measurements. The environments of Trp residues were also analyzed by fluorescence lifetime measurements. Three-exponential analysis of phase and modulation data gave excellent fits between experimental and theoretical curves as indicated by the low χ^2 values (see Table 2). The τ_i values and their fractional contributions represent lifetime distributions rather than lifetimes of individual residues. Even proteins with a single Trp residue have lifetime distributions that are attributed to protein dynamics, molecular interactions, and different Trp conformations in the peptide chain (*29*, *30*)

The results obtained for the Trp lifetimes (fractional and average) in the unlabeled forms, as well as the f_i values are similar for all the apoA-I variants. These results confirm that the average Trp environments are equivalent in the lipid-free forms of the proteins. Furthermore similar correlation times ($\phi_1 = 22.2-25.0$ ns, $\phi_2 = 0.18-0.26$ ns) indicate that the dimensions and the shapes of the lipid-free proteins are essentially the same. The one exception is the D9C-Ac form of apoA-I, which has a significantly longer global correlation time ($\phi_1 = 30.3$ ns), suggesting a more asymmetrical shape of this protein as compared with the other variants of apoA-I or an altered orientation of the Trp fluorophores with respect to the major axes of the molecule.

In addition to the structural properties of the lipid-free proteins, measured by spectroscopic methods, we examined their lipid-binding properties. All apoA-I variants formed rHDL particles of equal and uniform sizes (see Figure 1, panel B) with high efficiency. The proteins in the rHDL had very similar CD and fluorescence spectra (not shown). The same WMF (333 nm, Table 1) and similar average lifetime values (∼4.1 ns, Table 2) indicate that Trp environments in the unlabeled variants are also equivalent in the lipid-bound state. Rotational correlation times for the lipid-bound proteins were not measured because the lifetimes of the Trp and Ac fluorophores are too short to detect the global motions of the very large rHDL particles. The denaturation behavior of the lipid-bound proteins was identical as monitored by the changes in the wavelengths of maximum fluorescence of Ac as a function of GndHCl at equilibrium (see Figure 2, panel B).

Table 2: Trp Lifetimes and Rotational Correlation Times in Lipid-Free and rHDL Forms

protein	τ_1(ns)[a]	f_1[a]	τ_2 (ns)	f_2	τ_3 (ns)	f_3	$<\tau>$ (ns)[b]	χ^{2c}	ϕ_1 (ns)[d]	ϕ_2 (ns)	f_1	χ^{2e}
lipid-free												
WT	5.82	(0.29)	2.68	(0.54)	0.80	(0.17)	3.27	0.42	22.2	0.18	0.64	0.5
D9C	5.96	(0.32)	2.38	(0.53)	0.54	(0.15)	3.25	0.36	25.0	0.20	0.72	2.7
A232C	6.06	(0.29)	2.39	(0.59)	0.57	(0.12)	3.24	0.20	24.3	0.25	0.72	1.4
D9C-Ac	5.79	(0.29)	2.05	(0.47)	0.48	(0.24)	2.76	0.86	30.3	0.24	0.70	1.4
A232C-Ac	4.83	(0.35)	2.02	(0.52)	0.49	(0.13)	2.80	0.55	23.8	0.26	0.68	3.1
rHDL												
WT	6.91	(0.40)	2.55	(0.50)	0.48	(0.10)	4.09	0.52				
D9C	7.24	(0.39)	2.84	(0.48)	0.65	(0.13)	4.27	0.43				
A232C	6.85	(0.40)	2.71	(0.48)	0.69	(0.12)	4.12	0.32				
D9C-Ac	7.74	(0.26)	2.54	(0.50)	0.51	(0.24)	3.40	1.10				
A232C-Ac	5.94	(0.37)	2.44	(0.48)	0.53	(0.15)	3.45	1.35				

[a] Lifetimes (τ_i) and fractional contributions (f_i) from three-exponential analysis of time-resolved phase and modulation measurements. [b] Average lifetimes $<\tau>$ from five separate samples and experiments, calculated from $<\tau> = \tau_1 f_1 + \tau_2 f_2 + \tau_3 f_3$. [c] χ^2 is the reduced chi-square value for the fit to three discrete exponentials assuming errors of 0.2° and 0.02 for phase and modulation data, respectively. [d] ϕ_1 is the global rotational correlation time for the motion of the entire protein; ϕ_2 represents the average "local" motions of Trp; f_1 is the fractional contribution of ϕ_1. [e] χ^2 is the reduced chi-square value for the fit of the data to two discrete exponentials.

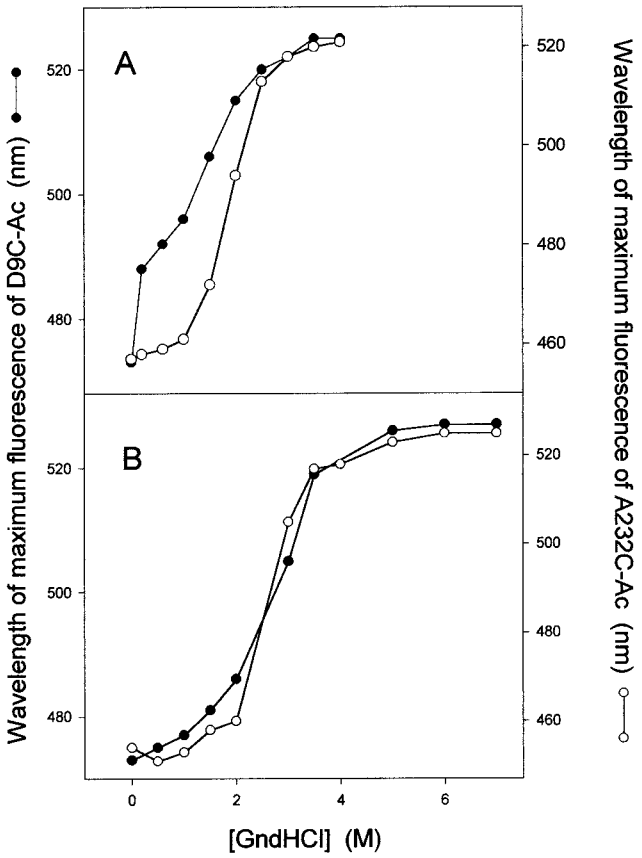

FIGURE 2: Denaturation curves for D9C-Ac (closed symbols) and A232C-Ac (open symbols) variants of apoA-I at equilibrium. Wavelengths of maximum fluorescence of the Ac probe are plotted as a function of [GndHCl]. (A) lipid-free proteins; (B) proteins in rHDL.

Another assay of the lipid-binding capacity of apoA-I is its ability to solubilize DMPC multilamellar liposomes at the phase transition temperature of this phospholipid (24 °C). In this study, we found no significant difference in the kinetics or efficiency of DMPC solubilization by any of the apoA-I variants (D9C, A232C, D9C-Ac, or A232C-Ac) as compared with plasma apoA-I or WT-proapoA-I (results not shown).

Structural Organization and Dynamic Properties of the N- and C-Terminal Domains. Having established the baseline properties of the D9C and A232C mutants and their adducts with acrylodan, D9C-Ac, and A232C-Ac, we proceeded to analyze the fluorescence results with the Ac probe in terms of the structures and motions of both extremes of the apoA-I molecule in solution.

The WMF values of acrylodan are 471 and 458 nm for D9C-Ac and A232C-Ac, respectively (Table 3). These WMF values compared with the range of Ac WMF values in solvents of different polarity—from 435 nm in dioxane to 530 nm in water (*31*)—indicate that the probe in both these regions is in hydrophobic environments. Table 3 also gives the corresponding lifetime values. A longer lifetime and a relatively blue-shifted WMF for the probe in position 232 indicate that the Ac in the C-terminal domain is more protected from solvent than in residue 9. Table 3 lists the correlation times for the Ac in both labeled species. The global correlation time (ϕ_1) for A232C-Ac (20.7 ns) is a little shorter than for the Trp residues (22.2−25.0 ns), suggesting that the region surrounding residue 232 may undergo some segmental motions. Nevertheless, the ϕ_1 values are comparable, indicating a high degree of local structure in the C-terminus. The global correlation time for D9C-Ac, (27.4 ns) is similar to the ϕ_1 measured for the Trp residues of this variant (30.3 ns) and supports the view that this protein form may be more asymmetrical than the WT protein and all other variants. Together these results indicate that there is a well-defined three-dimensional structure that keeps the probe in position 232 in a hydrophobic and relatively rigid environment.

In contrast to the very similar overall denaturation behavior of the lipid-free proteins measured by CD and WMF of Trp residues (not shown), the regions of apoA-I monitored specifically by the Ac probe in D9C-Ac and A232C-Ac have distinct denaturation curves (see Figure 2, panel A). The D9C-Ac protein has a biphasic denaturation profile, possibly due to the structural changes induced by the Ac probe, while the A232C-Ac variant exhibits a two-state behavior and has a curve with a midpoint at 2.0 M GndHCl and a calculated $\Delta G^\circ_{H_2O}$ of 4.0 kcal/mol. As compared to overall apoA-I denaturation, from CD or WMF measurements, having a midpoint at 1.4 M GndHCl and $\Delta G^\circ_{H_2O}$ of 2.5 kcal/mol, the A232C-Ac probe reports that the C-terminal region of apoA-I is more stable than the overall lipid-free apoA-I structure monitored by CD or Trp fluorescence measurements.

Table 3: Acrylodan WMF and Rotational Correlation Times in Lipid-Free and rHDL Forms

protein	WMF (nm)[a]	τ_1 (ns)[b]	f_1[b]	τ_2 (ns)	f_2	$<\tau>$[c] (ns)	χ^{2d}	ϕ_1 (ns)[e]	ϕ_2[e] (ns)	f_1[e]	χ^{2f}
lipid free											
D9C-Ac	471 ± 4	3.36	(0.81)	0.92	(0.19)	2.90	0.47	27.4	0.21	0.79	1.3
A232C-Ac	458	3.89	(0.84)	0.84	(0.16)	3.40	2.53	20.7	0.21	0.65	1.1
rHDL											
D9C-Ac	467 ± 4	3.71	(0.90)	0.86	(0.10)	3.43	0.74				
A232C-Ac	452	3.73	(0.91)	0.83	(0.09)	3.47	0.74				

[a] Wavelength of maximum fluorescence of acrylodan. [b] Lifetimes (τ_i) and fractional contributions (f_i) from two-exponential analysis of time-resolved phase and modulation measurements. [c] The average lifetimes $<\tau>$ from three separate samples and experiments, calculated from $<\tau> = \tau_1 f_1 + \tau_2 f_2$. [d] χ^2 is the reduced chi-square value for the fit to two discrete exponentials assuming errors of 0.2° and 0.02 for phase and modulation data, respectively. [e] ϕ_1 is the global rotational correlation time for the motion of the entire protein; ϕ_2 represents the average "local" motions of acrylodan; f_1 is the fractional contribution of ϕ_1. [f] χ^2 is the reduced chi-square value for the fit of the data to two discrete exponentials.

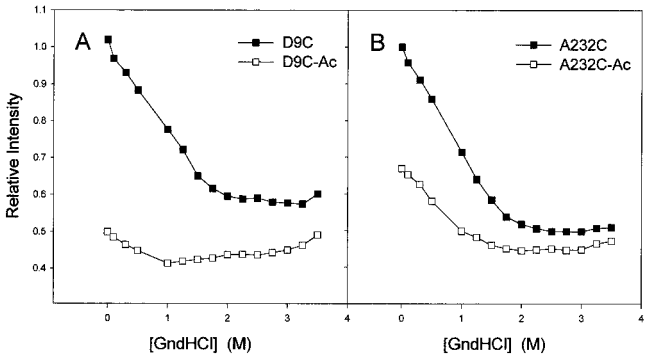

FIGURE 3: Denaturation curves of lipid-free variants of apoA-I (panel A: D9C and panel B: A232C), as monitored by Trp emission as a function of guanidine hydrochloride concentration. ApoA-I variants (0.1 mg/mL) were titrated with appropriate amounts of 6.4 M GndHCl stock solution and equilibrated during 10 min. Excitation wavelength was 295 nm; emission was integrated and corrected for dilution factors. Closed symbols show the emission of unlabeled forms and open symbols the emission for Ac-variants.

Upon binding of lipids in rHDL, the Ac probe in both positions experiences a 4−6 nm blue shift in WMF (Table 3) and an increase in the $<\tau>$, especially in the D9C-Ac. These data suggest that the environments of the probe in both extremes of the molecule become more hydrophobic, possibly due to contact with lipids.

Folding of ApoAI Variants. Energy Transfer in the Lipid-Free State. To obtain information on the folding of apoA-I in solution we measured the fluorescence energy transfer from the five Trp residues of the apoA-I variants located in the N-terminal half of the proapoA-I sequence (positions −3, 8, 50, 72, 108) to the Ac acceptor probe in position 9 or 232.

The decrease in the average fluorescence lifetimes and the integrated fluorescence intensities (Table 2, Figure 3) of Trp residues when the Ac probe is present on the same protein, strongly suggests resonance energy transfer from Trp residues to Ac. Other quenching effects due to structural changes and to solvent exposure in the Ac-labeled proteins are unlikely because of the demonstrated similarity in the protein structures and their spectral properties, especially for the A232C-Ac variant. Thus average distances (R) between the Trp residues and the Ac probe can be calculated from the efficiency of energy transfer (E) using fluorescence lifetime or intensity changes (eq 2). The calculated average distances are given in Table 4. The distances of 3.0−3.7 nm between the Ac probe in position 232 and the average Trp residue positions, indicate that the C-terminus folds back in space to come closer to the N-terminal half of the protein than would be expected from a maximum distance of about 15 nm for an elongated apoA-I monomer with overall dimensions of 15 × 2.5 nm (*32*). The calculated distances between the Ac probe in position 9 and the Trp residues are smaller than for the A232C-Ac variant because of the proximity of the probe in the sequence of proapoA-I to the Trp residues in positions −3 and 8; however, the relative orientation and steric effects of the proximal fluorophores may not be favorable for resonance energy transfer thus giving relatively long experimentally determined distances.

To further confirm the presence of energy transfer between the Trp residues and the Ac probe in both positions, we analyzed the changes in Trp fluorescence intensity during denaturation of the labeled proteins with increasing concentrations of GndHCl (Figure 3). As protein unfolding progresses, the difference in the Trp fluorescence intensity, in the presence and absence of Ac decreases. This means that the efficiency of energy transfer decreases due to increased separation of the fluorophores. Upon complete denaturation, at about 3 M GndHCl, the energy transfer in A232C-Ac becomes insignificant while some energy transfer persists in the D9C-Ac protein due to the proximity of the fluorophores in the primary sequence. Acrylodan fluorescence intensity as a function of denaturation by GndHCl of the lipid-free proteins (Figure 4) provides further evidence for energy transfer in the native proteins. The fluorescence intensity of Ac excited at 360 nm shows changes due to denaturation; however, the relative fluorescence intensity excited at 295 nm, with most of the intensity contributed by energy transfer from Trp residues, declines even more because of the increasing separation of the fluorophores. After complete denaturation, at about 3 M GndHCl, the fluorescence remaining for the D9C-Ac protein after excitation at 295 nm can be attributed to the residual energy transfer between proximal fluorophores in the linear sequence.

Finally, fluorescence lifetimes of Trp residues of the proteins labeled with Ac, in the presence and absence of denaturing amounts of GndHCl (Table 4), provide clear evidence for energy transfer between Trp and Ac fluorophores. The differences in lifetime values observed in the native state become much smaller in the denatured state.

Energy Transfer in rHDL. As described above for the lipid-free proteins, we calculated the distance from the average of the five Trp residues to the C-terminal region in the lipid-bound state using lifetime changes. An energy transfer efficiency of 16% (Table 4) indicated that the C-terminal 232 residue is relatively close to the N-terminal half of apoA-I in the discoidal complexes (~3.6 nm).

Table 4: Analysis of Fluorescence Resonance Energy Transfer for Lipid-Free Proteins and rHDL in the Absence and Presence of GndHCl

	lipid-free				rHDL			
	D9C	D9C-Ac	A232C	A232C-Ac	D9C	D9C-Ac	A232C	A232C-Ac
$<\tau>$ (ns)[a]	3.25	2.76	3.24	2.80	4.27	3.40	4.12	3.45
$<\tau>$ (+ GndHCl) (ns)[b]	2.99	2.95	3.04	3.05		2.84		2.79
E[c]		0.15		0.14		0.20		0.16
R (nm)[c]		3.6		3.7		3.4		3.6
F[a]	1.00	0.50	1.00	0.67				
F (+ GndHCl)[b]	0.60	0.49	0.51	0.47				
E[c]		0.50		0.33				
R (nm)[c]		2.7		3.0				

[a] Average lifetimes $<\tau>$ and fluorescence intensities (F) of Trp residues measured in the absence of GndHCl [b] Average lifetimes and fluorescence intensities of Trp residues measured in the presence of 3.5 M GndHCl for the lipid-free proteins and 7 M GndHCl for the proteins in rHDL particles, at equilibrium. [c] Efficiencies of energy transfer (E) and distances (R) calculated from $<\tau>$ and F values in the absence of GndHCl using the equation given in Materials and Methods.

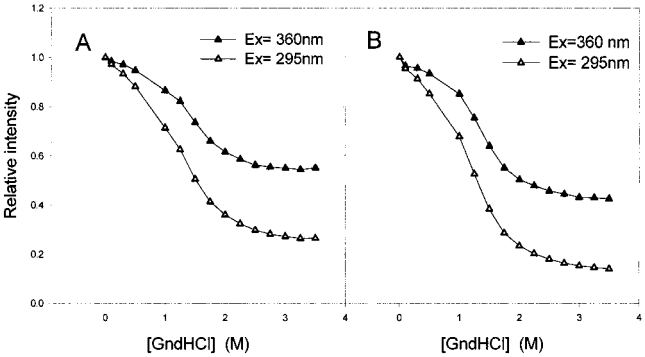

FIGURE 4: Changes in the integrated fluorescence intensity of Ac in Ac-labeled variants of apoA-I during denaturation with GndHCl (as described in Figure 3). Panel A: D9C-Ac; panel B: A232C-Ac. The Ac emission was recorded between 420 and 575 nm upon excitation at 360 nm (closed symbols) or 295 nm (open symbols). Intensities were normalized for better comparison.

Because of the long time necessary for equilibration during denaturation in the rHDL particles (~72 h), we were not able to perform intensity analysis combined with GndHCl denaturation but obtained lifetimes in the native rHDL and in the completely denatured forms (Table 4), confirming the presence of energy transfer.

DISCUSSION

In the spectroscopic experiments reported in this study, wild-type recombinant proapoA-I (WT-proapoA-I) was used as a control together with the mutant proapoA-I samples. Previous in vitro work from our laboratory (*21*) and from other groups (*33*) did not reveal any structural nor functional differences between plasma apoA-I and WT-proapoA-I.

An important prerequisite in this study of apoA-I mutants is that the structure and function of apoA-I be preserved upon mutation to introduce the Cys residues and their subsequent covalent modification with Ac. Our circular dichroism and fluorescence measurements have shown that the secondary and tertiary structure as well as the stability of the mutants and covalent adducts with Ac is very similar to wild-type proapoA-I. A possible exception is the D9C-Ac variant, which has a lower content of α-helix and a larger rotational correlation time as compared to the other protein forms. All proapoA-I variants are equally effective in solubilizing DMPC liposomes and in forming rHDL particles of the same size.

The absence of structural and functional effects of the point mutation (D9C) in the extreme N-terminal region of apoA-I is not surprising as naturally occurring mutants, P3R and P4R (*34*), as well as engineered mutants W-3F and W8F (*11*) do not affect the properties of apoA-I. Reported point mutations in the extreme C-terminal region of human apoA-I are relatively rare, but a single amino acid deletion (Glu 235) in the C-terminal domain was reported to impair the lipid binding properties of apoAI (*35*). Similarly, several point mutations especially designed to decrease the hydrophobicity of the eighth helical segment seem to impair the lipid-binding properties of apoA-I (*10*). However, the mutant constructed in this study, A232C, represents a conservative substitution in terms of bulk and polarity of the amino acids involved (*36*) and does not affect the structure nor the lipid-binding properties of apoA-I.

Covalent modification of -SH groups of proteins with fluorescent probes is a widely established approach for the study of the structure, dynamics, and functions of proteins (*37*). Of course, there is always a question regarding the effects of the probe itself on the properties of the protein. We addressed this issue by demonstrating that the A232C-Ac variant of the protein is indistinguishable in its structural and lipid-binding properties from plasma apoA-I and WT-proapoA-I.

On the other hand, the D9C-Ac form of the protein does have an altered α-helix content and shape as compared to control, indicating that the introduction of the aromatic probe by its bulk or chemical nature perturbs the structure of the lipid-free protein. However, the same apoA-I form (D9C-Ac) in the lipid-bound state regains the overall structure and stability of the native protein. Evidently, the structure of the lipid-bound protein depends more on protein−lipid interactions than on protein−protein contacts.

It should be mentioned here that there are two full-length natural Cys mutants of apoA-I: R173C (apoA-I-Milano) (*38*) and R151C (apoA-I-Paris) (*39*). These mutants occur in plasma, predominantly in disulfide-linked forms, including homodimers and heterodimers with apoA-II or apoE. As expected, the homodimeric mutants of apoA-I-Milano have quite different properties from plasma apoA-I in the lipid-free form (*40*) but bind lipid efficiently, forming rHDL products with altered diameters and different reactivities with lecithin cholesterol acyltransferase (*41*). In contrast, reduced and carboxymethylated apoA-I-Milano has structural and functional properties quite analogous to plasma apoA-I (*42*), as we find for the engineered Cys mutants in this study.

Time-resolved fluorescence anisotropy values for lipid-free proteins were measured either using Trp or Ac emission. Correlation times (ϕ_1 and ϕ_2) for Trp were obtained from this analysis (Table 2), using $<\tau>$ values. The longer correlation time, ϕ_1, corresponds to the global rotational motion of the lipid-free proteins; the subnanosecond ϕ_2 is interpreted as a measure of local torsional motions of the fluorophores. This is a common observation in soluble proteins, where local motions of Trp do occur as a result of normal structural fluctuations of the proteins (*37*).

The global correlation time from Trp fluorescence is 22.2 ns (average of 5 values). The ϕ_1 value for the D9C-Ac variant is different (30.3 ns) and probably represents a more asymmetrical protein form. The 22.2 ns global rotational correlation time is almost 2-fold greater than the correlation time calculated for a hydrated (0.3 g of H_2O/g of protein) sphere with the mass of apoA-I (12 ns) (*43*). This ratio of 1.85 corresponds to a prolate ellipsoid with an axial ratio of about 5:1 (*44*) and agrees well with viscometric and sedimentation velocity measurements reported previously that give overall dimensions of monomeric apoA-I of 2.5 × 15.0 nm (*32*, *45*). The global rotational correlation times determined from the Ac fluorescence anisotropy decay are comparable to those obtained for Trp (Table 3). It should be noted here that ϕ_1 values for Trp represent a weighted contribution of 5 residues, whereas the single Ac probe could be more sensitive to the rotation around one or the other major axis of the prolate ellipsoid representing the shape of the protein.

One of the main objectives of this work, was to obtain information on the structural organization of the C-terminal domain of apoA-I. While the N-terminal half of apoA-I is thought to be organized in a bundle of helices that stabilizes apoA-I in solution (*11*, *16*), there is no consensus about the structure at the C-terminus of apoA-I. From our previous deletion mutagenesis work (*13*), we concluded that the C-terminal half of the protein contains low amounts of secondary structure as compared to the N-terminal half of apoA-I. Also Roberts et al. (*16*) and Ji and Jonas (*14*) found that the sequence between amino acids 190−243 is highly susceptible to proteolysis. However, based on predictions from the primary sequence and circular dichroism measurements of apoA-I, Nolte and Atkinson propose an amphipatic helix extending from residue 231 to the C-terminus (*46*). The present results show that in addition, such a helix would have to make contacts with other protein regions to constitute a hydrophobic core large enough to sequester the Ac probe from solvent and to form a relatively stable local structure. This is consistent with the relatively high stability of the eighth helical-segment of apoA-I (residues 220−241) observed with synthetic peptides corresponding to the predicted amphipathic helices of apoA-I (*47*) and also with the higher $\Delta G^{\circ}_{H_2O}$ (4 kcal/mol) and midpoint of GndHCl concentration found in the denaturation of this domain (Figure 2, panel A). The regional difference in stability in the lipid-free Ac-labeled proteins is no longer present in the lipid-bound (rHDL) proteins measured soon after denaturant addition (not shown) or after equilibrium is attained (see Figure 2, panel B). Cooperative lipid binding apparently obliterates the local differences in protein stability.

Folding of Lipid-Free ApoA-I. From our fluorescence results, it is apparent that there is energy transfer between the Trp residues in the N-terminal half of apoA-I and Ac at position 232 in the sequence. The average distance calculated from the efficiency values is 3.0−3.7 nm. Taking into account the overall dimensions of a monomer of apoA-I (15 × 2.5 nm) (*32*), it appears that the protein folds back on itself to bring the C-terminus within 3.0−4.0 nm from at least one of the Trp residues of apoA-I. Trp residues located at distances greater than 5.0 nm would not contribute to energy transfer. From our previous work (*11*), we have observed that Trp residues cluster in lipid-free apoA-I leading to energy transfer among them. This homotransfer disappears in rHDL particles due to increased separation between the Trp residues upon binding to lipid. These and other spectroscopic results led us to propose that helices 1, 2, and 3 of apoA-I, containing Trp at positions 50, 72, and 108 (*47*), probably form part of a helix bundle in solution (*11*). This is in agreement with the results and conclusions of Rogers et al. (*45*) from hydrodynamic and proteolytic studies of apoA-I and structural analyses of the related chicken apoA-I (*48*) and apoE (*49*) soluble apolipoproteins. The X-ray structure by Borhani et al. (*7*) of the apoA-I truncated at the N-terminus is not relevant to the properties of a full-length monomer of apoA-I, in low salt solution, as discussed here.

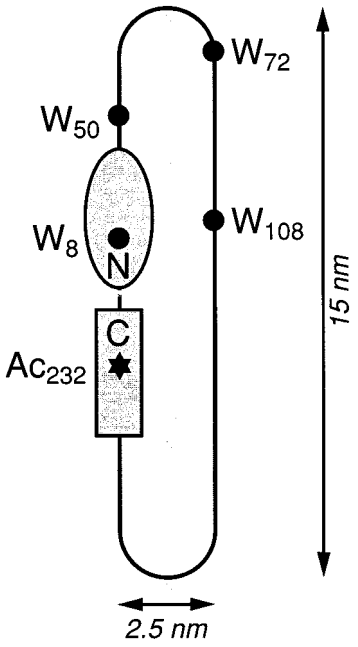

FIGURE 5: Schematic diagram of lipid-free apoA-I based on this study and results from published work (*11*−*14*, *32*, *45*, *46*). It includes compact N- and C-terminal regions of the protein (labeled N and C) that are adjacent to each other. The Trp residues (W_8, W_{50}, W_{72}, W_{108}) in the N-terminal half of the sequence are relatively near to each other (*11*, *13*) and to Ac_{232} in the C-terminal helix (residues 220−241) of apoA-I. The overall shape of the molecule is a rod with dimensions approximating 2.5 × 15 nm (*32*, *45*).

Unlike previous conclusions by Davidson et al. (*13*) and Rogers et al. (*45*), that the C-terminus of apoA-I is largely unstructured, we find that helix 8 (residues 220−241) and its immediate vicinity does have a relatively stable three-dimensional structure. Furthermore, the N- and C-termini of apoA-I move in concert with the entire macromolecule indicating a relatively condensed and rigid structure for the overall rodlike shape of the monomer.

On the basis of the observations made in this study and other work, we propose a general schematic organization of

lipid-free apoA-I as shown in Figure 5. In this diagram, the main constraints are (i) the shape of the molecule (*11*, *32*, *45*) about the width of two α-helices and the length of 3−4, 22-amino acid helical segments; (ii) the relative proximity of Trp residues to each other for energy transfer to take place (*11*) (W-3 not shown); (iii) the proximity (3−4 nm) of the C-terminal Ac_{232} probe to Trp residues; and (iv) the compact structures of the N- and C-terminal regions and overall rigid structure. The linear organization of apoA-I shown in Figure 5 satisfies these constraints and suggests that a helix−turn−helix encompasses the helices containing the Trp residues in positions 50, 72, and 108 (*11*). In the C-terminal half, helices corresponding to residues 121−142 and 220−241 probably help organize the structure (*12*, *13*).

Folding of ApoA-I in rHDL. In the lipid-bound, rHDL state, the C-terminal Ac probe is near (∼3.6 nm) to one or more Trp residues; therefore, models for the organization of two apoA-I molecules in a discoidal rHDL should take this constraint into consideration. In the "picket fence" model of discoidal rHDL, the N-terminal half of each apoA-I monomer is distant from its own C-terminus (>5.0 nm); therefore, intramolecular energy transfer between the Trp residues and the Ac acceptor on the same apoA-I molecule would be insignificant. Only intermolecular energy transfer between the two apoA-I molecules would be expected. In the "belt" model, both intra- and intermolecular energy transfer could occur. Keeping this restriction in mind, only the "picket-fence" head-to-head configuration (*50*) appears to be excluded as the principal configuration of two apoA-I molecules in rHDL based on our energy transfer results.

Finally, it should be noted that while our energy transfer results lead to interesting predictions about the structure of apoA-I in the lipid-free and lipid-bound states, experiments using single Trp mutants of apoA-I (*11*) in conjunction with the Ac probe would yield more precise distance information. Such experiments are underway in our laboratory.

REFERENCES

1. Fielding, C. J., Shore, V. G., and Fielding, P. E. (1972) *Biochem. Biophys. Res. Commun. 46*, 1493−1498.
2. Rye, K.-A. and Barter, P. J. (1992) in *Structure and Function of Apolipoproteins* (Rosseneu, M., Ed.), pp 401−426, CRC Press, Boca Raton.
3. Pussinen, P. J., Jauhiainen, M., Metso, J., Pyle, L. E., Marcel, Y. L., Fidge, N. H., and Ehnholm, C. (1998) *J. Lipid Res. 39*, 152−161.
4. Fidge, N. H. (1999) *J. Lipid Res. 40*, 187−201.
5. Segrest, J. P., Jones, M. K., De Loof, H., Brouillete, C. G., Venkatachalapathi, Y. V., and Anantharamaiah, G. M. (1992) *J. Lipid Res. 33*, 141−166.
6. Jonas, A., Hefele Wald, J., Harms Toohill, K. L., Krul, E. S., and Kézdy, K. E. (1990) *J. Biol. Chem. 265*, 22123−22129.
7. Borhani, D. W., Rogers, D. P., Engler, J. A., and Brouillette, C. G. (1997) *Proc. Natl. Acad. Sci. 94*, 12291−12296.
8. Minnich, A., Collet, X., Roghani, A., Cladaras, C., Hamilton, R. L., Fielding, C. J., and Zannis, V. I. (1992) *J. Biol. Chem. 267*, 16553−16560.
9. Sorci-Thomas, M., Kearns, M. W., and Lee, J. P. (1993) *J. Biol. Chem. 268*, 21403−21409.
10. Laccotripe, M., Makrides, S. C., Jonas, A., and Zannis, V. (1997) *J. Biol. Chem. 272*, 17511−17522.
11. Davidson, W. S., Arnvig-McGuire, A., Kennedy, A., Kosman, J., Hazlett, T. L., and Jonas, A. (1999) *Biochemistry 38*, 14387−14395.
12. Mishra V. K., Palgunachari, M. N., Datta, G., Phillips, M. C., Lund-Katz, S., Adeyeye, S. O., Segrest, J. P., and Anantharamaiah, G. M. (1998) *Biochemistry 37*, 10313−10324.
13. Davidson, W. S., Hazlett, T., Mantulin, W. W., and Jonas A. (1996) *Proc. Natl. Acad. Sci. U.S.A. 93*, 13605−13610.
14. Ji, Y. and Jonas, A. (1995) *J. Biol. Chem. 270*, 11290−11297.
15. Morrison, J., Fidge, N. H., and Tozuka, M. (1991) *J. Biol. Chem. 266*, 18780−18785.
16. Roberts, L. M., Ray, M. J., Shih, T−W., Hayden, E., Reader, M. M., and Broulliette, C. G. (1997) *Biochemistry* 36, 7615−7624.
17. Leroy, A. and Jonas, A. (1994) *Biochim. Biophys. Acta. 1212*, 285−294.
18. Haugland, R. P. (1996) in *Handbook of Fluorescent Probes and Research Chemicals*, 6th ed., pp 55−58, Molecular Probes, Eugene, OR.
19. Lowry, O. H., Rosebrough, N. J., Farr, A. L., and Randall, R. J. (1951) *J. Biol. Chem. 193*, 265−275.
20. Durbin, D. M., and Jonas A. (1997) *J. Biol. Chem. 272*, 31333−31339.
21. McGuire, K. A., Davidson, W. S., and Jonas, A. (1996) *J. Lipid Res. 37*, 1519−1528.
22. Chen, Y.-H., Yang, J. T., and Martinez, H. (1972) *Biochemistry 11*, 4120−4131.
23. Greene, R. F. and Pace, C. N. (1974) *J. Biol. Chem. 249*, 5388−5393.
24. Pace, C. N. (1975) *CRC Crit. Rev. Biochem. 3*, 1−43.
25. Spencer, R. D., and Weber, G. (1970) *J. Chem. Phys. 52*, 1654−1663.
26. Thompson, R. B., and Gratton, E. (1988) *Anal. Biochem. 60*, 670−674.
27. Lakowicz, J. R. (1986) in *Principles of Fluorescence Spectroscopy*, 3rd ed., pp 305−309, Plenum Press, New York and London.
28. Kulwinder, F., Brennan, J. D., Baker, G. A., Doody, M. A., and Bright, F. V. (1998) *Biophys. J. 75*, 1084−1096.
29. Weber, G. (1977) *J. Chem. Phys. 66*, 4081−4091.
30. Helms, M. K., Hazlett, T. L., Mizuguchi, H., Hasemann, C. A., Uyeda, K., and Jameson, D. M. (1998) *Biochemistry 37*, 14057−14064.
31. Prendergast, F. G., Meyer, M., Carlson, G. L., Iida, S., and Potter, J. D. (1983) *J. Biol. Chem. 258*, 7541−7544.
32. Barbeau, D. L., Jonas, A. Teng, T.-I., and Scanu, A. (1979) *Biochemistry 18*, 362−369.
33. Sorci-Thomas, M. G., Parks, J. S., Kearns, M. W., Pate, G. N., Zhang, C., and Thomas, M. J. (1996) *J. Lipid Res. 37*, 673−683.
34. Jonas, A., von Eckardstein, A., Kézdy, K. E., Steinmetz, A., and Assmann, G. (1991) *J. Lipid Res. 32*, 97−106.
35. Huang, W., Sasaki, J., Matsunaga, A., Han, H., Li, W., Koga, T., Kugi, M., Ando, S., and Arakawa, K. (2000) *Arterio. Thromb. Vasc. Biol. 20*, 210−217.
36. Wimley, W. C. and White, S. H. (1996) *Nat. Struct. Biol. 3*, 842−848.
37. Hamman, B., Oleinikov, A. V., Jokhadze, G. G., Traut, R. R., and Jameson, D. M. (1996) *Biochemistry 35*, 16672−16679.
38. Franceschini, G., Sirtori, C. R., Capurso, A., Weisgraber, K. H., and Mahley, R. W. (1980) *J. Clin. Invest. 66*, 892−900.
39. Bruckert, E., von Eckardstein, A., Funke, H., Beucler, I., Wiebusch, H., Turpin, G., and Assmann, G. (1997) *Atherosclerosis 128*, 121−128.
40. Calabresi, L., Vecchio, G., Longhi, R., Gianazza, E., Palm, G., Wadensten, H., Hammarstrom, A., Olsson, A., Karlstrom, A., Sejlitz, T., Ageland, H., Sirtori, C. R., and Franceschini, G. (1994) *J. Biol. Chem. 269*, 32168−32174.
41. Calabresi, L., Vecchio, G., Frigerio, F., Vavassori, L., Sirtori, C. R., and Franceschini, G. (1997) *Biochemistry 36*, 12428−12433.
42. Suurkuusk, M., and Hallen, D. (1999) *Eur. J. Biochem. 265*, 346−352.
43. Sanchez, S. A., Hazlett, T. L., Brunet, J. E., and Jameson, D. M. (1998) *Protein Sci. 7*, 2184−2189.

44. Weber, G. (1953) *Adv. Protein. Chem. 8*, 415−459.
45. Rogers, D. P., Roberts, L. M., Lebowitz, J., Engler, J. A., and Brouillette, C. G. (1998) *Biochemistry 37*, 945−955
46. Nolte, R. T., and Atkinson, D. (1992) *Biophys. J. 63*, 1221−1239.
47. Palgunachari, M., Mishra, V. K., Lund-Katz, S., Phillips, M. C., Adeyeye, S. O., Anatharamaiah, G. M., and Segrest, J. P. (1996) *Arterio. Thromb. Vasc. Biol. 16*, 328−338.
48. Kiss, R. S., Kay, C. M., and Ryan, R. O. (1999) *Biochemistry 38*, 4327−4334.
49. Wilson, C., Wardell, M. R., Weisgraber, K. H., Mahley, R. W., and Agard, D. A. (1991) *Science 252*, 1817−1822.
50. Phillips, J. C., Wriggers, W., Li, Z., Jonas, A., and Schulten, K. (1997) *Biophys. J. 73*, 2337−2346.

BI0014251